

# Quantum interference in resonant Raman spectra of I<sub>2</sub> in condensed media

M. Ovchinnikov and V. A. Apkarian

Department of Chemistry, University of California, Irvine, California 92697-2025

(Received 13 December 1996; accepted 24 January 1997)

Both  $B(^3\Pi_{u0})$  and  $B''(^1\Pi_{1u})$  surfaces contribute to resonance Raman scattering of iodine, and the interference between these two channels leads to modulation of the intensity profile of overtone progressions, as observed experimentally. The effect is simulated through mixed order semiclassical molecular dynamics. © 1997 American Institute of Physics. [S0021-9606(97)02613-5]

## I. INTRODUCTION

Resonance Raman (RR) spectra of I<sub>2</sub> in condensed media, in solid rare gases,<sup>1,2</sup> and in liquids,<sup>3-5</sup> and in particular in liquid Xe,<sup>4</sup> and CCl<sub>4</sub>,<sup>5</sup> have recently been revisited with the aims of extracting dynamical information on ultrafast time scales.<sup>2-8</sup> The spectra contain long overtone progressions which do not decay monotonically. If properly interpreted, the intensity profiles of the progressions can in principle elucidate dynamics that proceeds on time scales shorter than those commonly accessible in direct time domain measurements. A rigorous interpretation of such spectra requires the analysis of the quantum many-body correlations that define the RR observable. Quite recently we introduced such a method, namely, mixed order semiclassical molecular dynamics, which allows the rigorous computation of time dependent quantum amplitudes of systems of large dimensionality.<sup>8</sup> While in the form introduced the method is accurate for relatively short times, its limit of accuracy far exceeds the relevant time scale of RR scattering of <150 fs in these systems. As a demonstration of the method, we already applied it to simulations of RR spectra in solid Kr, taking the single  $B(^3\Pi_{0u}^+)$  state into account. We noted then that the deviations observed between simulation and experiment could not be reconciled with single surface dynamics. Further, we noted that at the wavelengths of interest, there are two Raman active surfaces present in I<sub>2</sub> as illustrated in Fig. 1. These are the bound  $B(^3\Pi_{0u}^+)$  state and the repulsive  $B''(^1\Pi_{1u})$  state, both of which are dipole allowed transition from the ground,  $X(^1\Sigma_g^+)$ , state.<sup>9</sup> Interference between these two Raman scattering channels will occur and should be taken into account in spectral analyses. Here we show that this effect explains the experimentally observed non monotonic decay of intensities in the overtone progression of I<sub>2</sub> in solid Kr. A more extended analysis of experiments in both solids and liquids we reserve for a future publication.<sup>10</sup>

## II. THEORY

The time dependent interpretation of RR spectra involves a three-time correlation function.<sup>11</sup> If we forgo the linewidth information contained in the time correlation between the excited state wave packet and the vibrational overtones in the final ground state, it is possible to obtain the scattering intensities as

$$I(\omega_n) = \omega_n^e \omega \sum_k e^{-\beta E_k} \left| \int e^{i\omega t} \langle \psi'_k(R, \{r_i\}; t) | \right. \\ \left. \times \psi''_n(R) \psi''_k(\{r_i\}) \rangle dt \right|^2 \quad (1a)$$

$$= \omega_n^3 \omega \left| \int e^{i\omega t} \text{Tr}(\rho_n(R', R'', \{r_i, r_i''\}; t)) dt \right|^2 \quad (1b)$$

$$= \omega_n^3 \omega \left| \int e^{i\omega t} C_n(t) dt \right|^2 \quad (1c)$$

in which  $\omega$  is the excitation laser frequency,  $\omega_n$  is the frequency for scattering in the  $n$ th overtone, prime and double prime indicate excited and ground electronic states,  $R$  is the I<sub>2</sub> coordinate, and  $r_i$  represent solvent coordinates. In the mixed order semiclassical treatment, the initial density matrix on the  $X$  ground state

$$\rho_n(R', R'', \{r_i', r_i''\}; 0) = \psi_n^*(R'') \rho_0(\{r_i', r_i''\}) \quad (2)$$

is propagated on the excited surface using propagators in initial value representation.<sup>12</sup> The Van Vleck propagator,<sup>13</sup> which corresponds to the stationary phase approximation in second order, is used to propagate the extremely anharmonic I<sub>2</sub> coordinate in the excited state; while the zeroth order propagator is used for the solvent coordinates.<sup>8</sup> Although the many-body wave function is sampled and propagated, to forgo the computationally intensive procedure of a second time correlation, the evolving amplitude is projected on the vibrational eigenstates of I<sub>2</sub>( $X$ ), effectively assuming separation between solute and solvent coordinates in the final scattering state as emphasized in Eq. (1a).

The two channel scattering we consider under the assumption that there is no electronic coupling between  $B$  and  $B''$  surfaces. Accordingly, we independently propagate the initial density on both surfaces, and then carry out the correlation where now in terms of the many-body wave packets:

$$\langle \psi'_k(R, \{r_i\}; t) | = |\mu_{BX}|^2 \langle \psi_k^B(R, \{r_i\}; t) | \\ + |\mu_{B''X}|^2 \langle \psi_k^{B''}(R, \{r_i\}; t) | \quad (3)$$

and the known transition dipole moments of  $B \leftarrow X$  and  $B'' \leftarrow X$  are used for the relative weight of each channel, neglecting their coordinate dependence.<sup>9</sup> The details of the simulations have already been discussed.<sup>8</sup> We use the anisotropic I<sub>2</sub>-Kr potentials for the ground state, while in the excited state we use pairwise additive isotropic I-Kr inter-

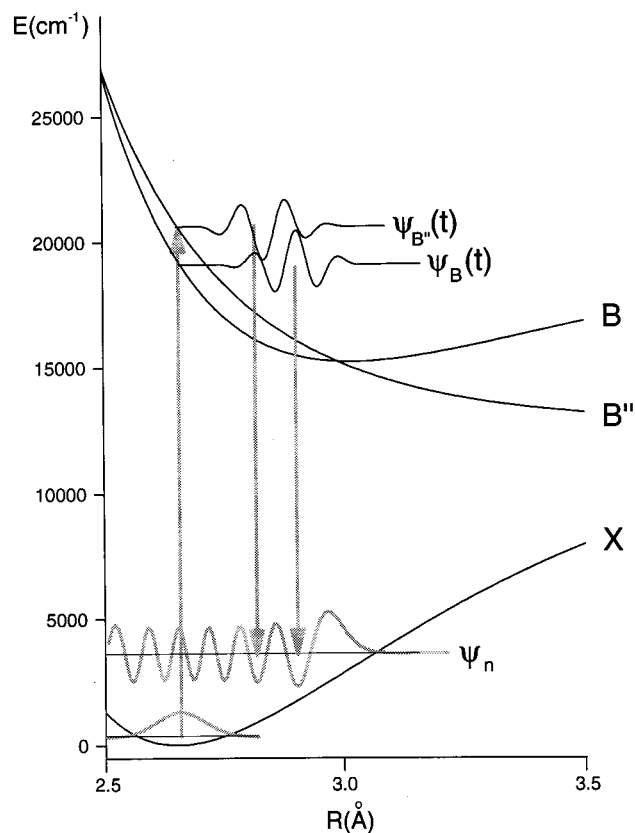


FIG. 1. Relevant energy diagram. RR scattering from two different time dependent packets to the same final state leads to interference.

actions with the Lennard-Jones parameters of Xe–Kr.<sup>14</sup> The I–I interactions in the  $X$  and  $B$  states are taken as Morse functions, while for the  $B''$  state we use the form suitable at short distances<sup>9</sup>

$$V_{B''}(R) = \frac{8.61 \times 10^7}{R^{9.5}} + 12580 \quad (\text{in units of cm}^{-1} \text{ and } \text{Å}) \quad (4)$$

recognizing that the details of the potential at  $R > 3.2$  Å are of no consequence; since, as already discussed, the bath correlation function decays near  $t = 100$  fs, prior to  $I_2$  reaching these distances. The results to be reported are for a simulation cell containing 100 atoms, subject to periodic boundary conditions, and for an ensemble of 25 600 trajectories (a grid of  $160 \times 160$  in  $p, q$  space is sampled) propagated on each of the electronic surfaces  $X$ ,  $B$ , and  $B''$ .

### III. RESULTS AND DISCUSSION

The results of the simulation for 488 nm excitation of  $I_2$  isolated in solid Kr, are compared with experiment in Fig. 2 (all intensities are normalized to  $\nu = 1$ ). After an initial monotonic decay, the experimental intensity profile shows a plateau between  $\nu = 10$  and 20, with a slight dip near  $\nu = 9$ . This profile cannot be reproduced with single surface dynamics, when considering the  $B$  state alone, as illustrated in Fig. 2(a). A nearly exact reproduction of the profile is ob-

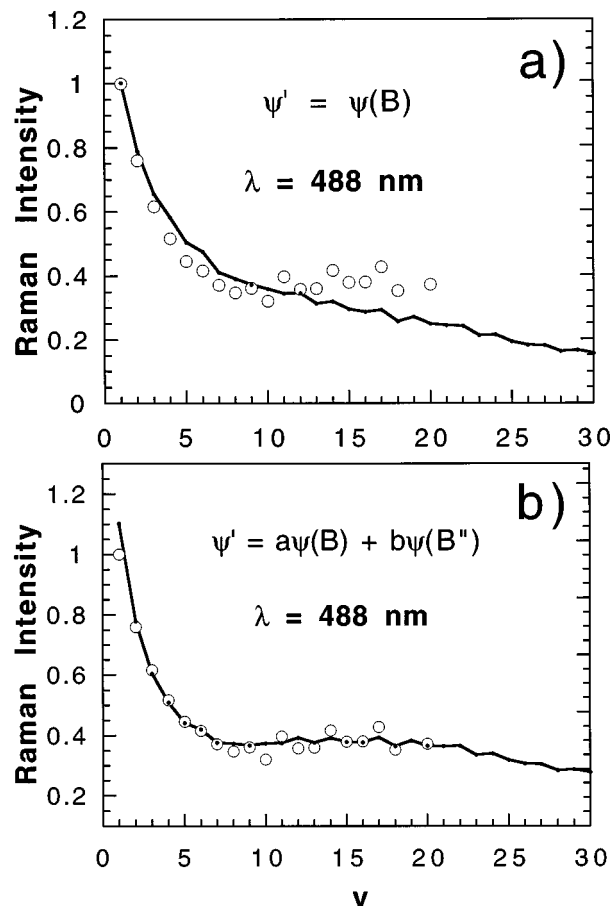


FIG. 2. Comparison between experiment and simulation. Top panel: single surface simulations; bottom panel; two-surface simulations. Note the change in ordinate scale between the two panels.

tained in the two-channel scattering, as illustrated in Fig. 2(b). To show the good agreement in profiles, in the comparison of Fig. 2(b) we have introduced a 10% offset in the ordinate. This shift could be interpreted as either uncertainty in the  $\nu = 1$  scattering intensity, or the improper subtraction of the incoherent fluorescence background present in the solid state spectra (for the raw spectra see Refs. 1 and 2). The nearly perfect agreement is somewhat fortuitous, since the simulations are carried out within the Condon approximation of constant transition dipoles. The more significant result is that the observed nonmonotonic decay profiles arise naturally from interference due to two Raman scattering channels.

In Fig. 3, we provide the RR scattering probabilities from individual channels, along with the two-channel results. Despite the fact that at this wavelength the RR scattering probability from  $B''$  alone is only  $\sim 3\%$  of that from  $B$ , the interference between the two channels produces a significant modulation of the overall signal. At  $\nu = 1$ , the interference is partially constructive, and the net scattering probability is higher than the  $B$  channel alone. The interference is destructive between  $\nu = 2$  and  $\nu = 15$ , and remains constructive above  $\nu = 15$ . Inspection of the correlation functions from each of the channels to the same final scattering state,  $C_n(t)$ , which is shown in Fig. 4, supports this picture. While

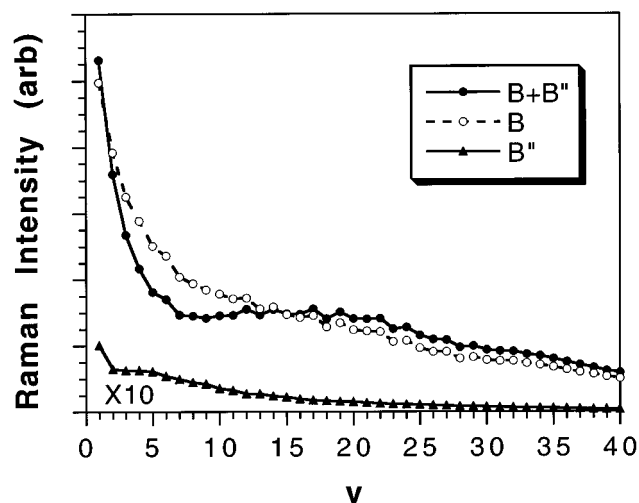


FIG. 3. Simulations of RR intensities from  $B$  and  $B''$  channels individually, and as a two-channel system.

for the Rayleigh peak, for  $v=0$ , the two-channel scattering is necessarily constructive, already for  $v=1$  the interference is only partially constructive. For  $v=9$  where the most complete destructive interference occurs the correlations are out of phase, and near  $v=26$  the correlations are in phase and therefore the interference is constructive. Note, the contribution from each channel is weighted by its integrated absorption coefficient, 1:3.7 for  $B'':B$ , and therefore only partial interference is possible [see Eq. (2)]. The squared Fourier transform of the correlation yields the scattered intensity [see Eq. (1)], accordingly, where the scattering probability from  $B''$  alone is 3%, as much as 10% modulation of the overall intensity through interference can occur.

The general features of this two-channel interference are predictable. In the case of low overtones, where the envelope of the packet has not yet spread in time (or space), the interference conditions are derived mainly from the separation between the repulsive walls of the two electronic surfaces (the Fourier transform acquires an additional beat due to detuning  $\Delta E/h$ , where  $\Delta E$  is the vertical separation between the two potentials). If the two surfaces are not exactly parallel, then the interference pattern will depend on excitation wavelength. It is only for these low lying overtones, where the phase velocity and spread of the wave packet are comparable, that one expects the Raman intensity profile to be modulated rapidly, from one overtone to the next. In the present example, from fully constructive at  $v=0$ , the interference becomes destructive already at  $v=2$ . In contrast, in the case of higher overtones both separation between surfaces and their curvatures determine the interference patterns, since now significant phase accumulates due to evolving dynamics. However, now the intensity would be expected to be only slowly modulated, as in the range between  $v=9$  and 30 in Fig. 2, since now the envelopes of the correlation functions are significantly broader in time than their internal phase structure (compare  $v=1$  to  $v=26$  in Fig. 4). The small oscillations observed on the simulated profile around  $v=20$  are not real. They are the result of statistical

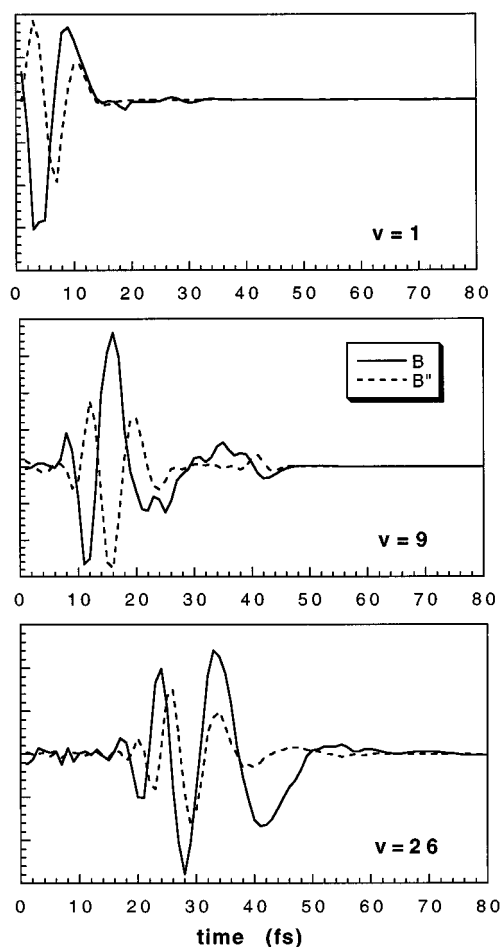


FIG. 4. Correlation functions,  $C_v(t)$ , for scattering into particular final eigenstates of  $I_2$ . Partial, destructive, and constructive interferences, are illustrated for  $v=1$ ,  $v=9$ , and  $v=26$ , respectively.

noise as verified by the fact that when a smaller ensemble of trajectories is considered this noise grows. Similarly, the oscillations observed in the experiment in this range, are ascribed to experimental error.

With the exception of the time dependent self-consistent field (TDSCF) treatment of Jungwirth and Gerber,<sup>7</sup> starting with the work of Kono and Lin,<sup>6</sup> up to the most recent liquid phase treatments,<sup>5</sup> analyses of the RR spectra of  $I_2$  in condensed media have relied on one-dimensional simulations, on a single electronic surface, with a phenomenological wavelength dependent damping constant used to account for all couplings to the bath. We have discussed some of the pitfalls of such analyses.<sup>8</sup> In particular, the decay of the many-body correlations are neither exponential nor determined by excitation wavelengths, but rather a sensitive function of the assumed interaction potentials and their associated early time many-body dynamics. On the time scale of the decay of the bath correlation of  $\sim 100$  fs in this case (see Fig. 13 in Ref. 8), no recursions of the packet evolving on the  $B$  surface occur. Thus, none of the features in the RR spectra can be attributed to interference between the outgoing and incoming packets on the  $B$  surface. Moreover, the nearly exact reproduction of the RR profile here, would im-

ply that nonadiabatic dynamics due to the various crossings of  $B$  with other electronic surfaces, and in particular between  $B$  and  $B''$ , is negligible. The single surface TDSF calculations are also in agreement with this conclusion.<sup>7</sup> This aspect was more directly demonstrated in time domain measurements in solid Kr.<sup>15</sup> We had in the past speculated that the structure in the RR spectra in solid rare gases may arise from coupling to a local phonon and that the abrupt termination of intensities may signify a sudden curve crossing.<sup>2</sup> With the present interpretation of the structure in the overtone intensity profile, and the time domain measurements in solid Kr, we now know that those speculations were incorrect. The structure naturally arises as a result of interference between the two active Raman scattering surfaces of  $B$  and  $B''$ , and the termination of the progression near  $v=20$  is experimental in origin, due to the very strong incoherent fluorescence background that overtakes the RR signal.<sup>1,2</sup>

Ultrafast nonadiabatic dynamics on the time scale of 30 fs, and partial recursions on the  $B$  state, are offered to explain the features of RR spectra in liquid  $\text{CCl}_4$  and liquid Xe.<sup>4,5</sup> These arguments are in part supported by recent simulations of nonadiabatic dynamics in these systems.<sup>16,17</sup> While indeed there are important differences between solid Kr vs solid Xe,<sup>18</sup> and solid vs liquid phases,<sup>19</sup> the predissociation dynamics on the sub-100 fs time scale, is less of an issue. Yet, the interference effect considered here is present in all media, and should be carefully considered first, prior to invoking other explanations for the observed structure in the RR spectra.

#### IV. CONCLUSIONS

The nonmonotonic decay of RR intensities in the overtone progression of  $\text{I}_2$  isolated in solid Kr can be nearly exactly reproduced by consideration of the interference between two scattering channels, RR scattering from  $B$  and  $B''$  states. This analysis is made possible by the mixed order semiclassical molecular dynamics simulations, which allow the calculation of many-body quantum time correlation functions for the time scales of relevance.<sup>8</sup> The analysis yields a detailed description of the dynamics in this particular case for the first 100 fs. The subsequent dynamics out to  $\sim 10$  ps has also been obtained through time domain measurements,<sup>15</sup> and a rather complete picture for this system now exists. In solid Kr, predissociation of  $\text{I}_2(B)$  occurs on the time scale of  $\sim 5$  ps, and throughout this period the classical coherence of the system is maintained. The latter aspect has been put to the more rigorous test of preparation with chirped pulses, and it has been shown that the system retains memory of the

coherence of the pump laser pulse for more than 15 vibrational periods, until it decays through predissociation.<sup>20</sup> While there are important differences in dynamics of  $\text{I}_2$  in liquids and in Xe, these differences are not expected to be significant on time scales  $< 100$  fs to effect RR profiles. A careful analysis of interferences in the RR spectra of these systems may, however, yield exquisitely detailed information about differential solvation of the repulsive walls of  $B$  and  $B''$  potentials.

#### ACKNOWLEDGMENTS

We gratefully acknowledge the support by AFOSR, under a University Research Initiative Grant No. F49620-1-0251, which made this work possible. Discussions with N. Schwentner, and preprints of Refs. 5 and 16 received during the preparation of this manuscript, have been quite stimulating.

- <sup>1</sup>W. F. Howard and L. Andrews, *J. Raman Spectrosc.* **2**, 447 (1974); Grzybowski and L. Andrews, *ibid.* **4**, 99 (1975).
- <sup>2</sup>v. A. Apkarian, in *Femtochemistry, Ultrafast Chemical and Physical Processes in Molecular Systems*, edited by M. Chergui (World Scientific, Singapore, 1996), p. 603.
- <sup>3</sup>R. J. Sension and H. L. Strauss, *J. Chem. Phys.* **85**, 3791 (1986); **87**, 6221 (1987); R. J. Sension, T. Kobayashi, and H. L. Strauss, *ibid.* **87**, 6233 (1987); R. J. Sension and H. L. Strauss, *ibid.* **88**, 2289 (1988).
- <sup>4</sup>J. Xu, N. Schwentner, and M. Chergui, *J. Chem. Phys.* **101**, 7381 (1994); J. Xu *et al.*, *J. de Chim. Phys.* **92**, 541 (1995).
- <sup>5</sup>J. Xu *et al.*, *J. Raman Spectrosc.* (in press).
- <sup>6</sup>H. Kono and S. H. Lin, *J. Chem. Phys.* **84**, 1071 (1986).
- <sup>7</sup>P. Jungwirth and R. B. Gerber, *J. Chem. Phys.* **102**, 8855 (1995); P. Jungwirth, E. Fredj, and R. B. Gerber, *ibid.* **104**, 9332 (1996).
- <sup>8</sup>M. Ovchinnikov and V. A. Apkarian, *J. Chem. Phys.* **105**, 10312 (1996).
- <sup>9</sup>J. Tellinghuisen, *J. Chem. Phys.* **76**, 4736 (1982).
- <sup>10</sup>K. Kizer, M. Ovchinnikov, and V. A. Apkarian (in preparation).
- <sup>11</sup>S. Mukamel, *Principles of Nonlinear Optical Spectroscopy* (Oxford University Press, New York, 1995).
- <sup>12</sup>A rather thorough discussion of the semiclassical approach to computation of condensed phase quantum time correlation functions was given by J. Cao and G. V. Voth, *J. Chem. Phys.* **104**, 273 (1996).
- <sup>13</sup>J. H. Van Vleck, *Proc. Natl. Acad. Sci.* **14**, 178 (1928).
- <sup>14</sup>For a clear discussion of the justification of these potentials, see F. Yu. Naumkin and P. J. Knowles, *J. Chem. Phys.* **103**, 3392 (1995).
- <sup>15</sup>R. Zadoyan, M. Sterling, and V. A. Apkarian, *J. Chem. Soc. Faraday Trans.* **92**, 1821 (1996).
- <sup>16</sup>V. S. Batista and D. F. Coker, *J. Chem. Phys.* **105**, 4033 (1996); (submitted).
- <sup>17</sup>M. Ben-Nun and R. D. Levine, *Chem. Phys.* **201**, 163 (1995); M. Ben-Nun, R. D. Levine, and G. R. Fleming, *J. Chem. Phys.* **105**, 3035 (1996).
- <sup>18</sup>Time domain measurements in Ar, Kr, and Xe have recently been completed in our laboratory. In contrast with Ar and Kr, in Xe the  $B$  state is subject to a strong avoided crossing, which leads to fast predissociation at excitation wavelengths shorter than 545 nm.
- <sup>19</sup>N. F. Scherer, D. M. Jonas, and G. R. Fleming, *J. Chem. Phys.* **99**, 153 (1993).
- <sup>20</sup>C. J. Bardeen *et al.*, *J. Chem. Phys.* (to be published).